

Interatomic transitions and relaxation effects in Auger spectra of several gas adsorbates on transition metals

M. Salmerón,* A. M. Baró, and J. M. Rojo

Departamento de Física Fundamental, Universidad Autónoma de Madrid, Canto Blanco, Madrid, Spain

(Received 24 November 1975)

A systematic investigation of the fine structure of adsorbate peaks in Auger spectra is presented. Spectra of a wide range of systems involving carbon, sulphur, oxygen, chlorine, and nitrogen adsorbates on copper, nickel, iron, and zinc substrates are reported with a resolution $\Delta E/E \sim 0.006$. According to a previous suggestion two types of transitions are identified and separated in such spectra. Interatomic transitions involve deexcitation of the initial adsorbate core hole from electrons in the substrate valence band. These transitions are rather similar to the ones involved in ion neutralization spectroscopy and are relatively unperturbed by final-state effects. Intra-atomic transitions show the same type of perturbation already observed in other investigations of Auger spectra involving rather localized valence bands, like *d* bands in transition metals. We identify peaks associated to spectral terms corresponding to final-state configuration interaction. Measurements of the energy of these peaks are used, in connection with photoemission binding energies of other authors, for calculating energy shifts. These shifts are then tentatively analyzed in terms of relaxation energies and, particular, extra-atomic relaxation energies are estimated. A discussion of the general conditions for correlating Auger-electron data and valence-band density of states is offered.

I. INTRODUCTION

Auger electron spectroscopy (AES) is currently used as a sensitive probe of the surface chemical composition. Much controversy has arisen, on the other hand, following the original suggestion by Lander¹ that information about the density of states (DOS) could be extracted from the line-shape analysis of Auger peaks involving valence-band levels. It is worth remarking that the use of AES as a valence-band spectroscopy in the neighborhood of the surface would result in a number of benefits. For example, the high scanning speed of AES, as compared to techniques involving photons, could be useful for tracking fast reactions or for studying surfaces with a high contamination rate. Moreover, most surface research systems have Auger detection capabilities and, consequently, probing the electron levels could be performed routinely as a further input in surface studies.

Several attempts have been already made in order to explore this possibility of AES.²⁻⁹ However, an unambiguous correlation between line-shape data of Auger spectra involving valence-band levels and DOS has been obtained only in very few cases. In order to clarify this correlation it is convenient to classify the previous experimental results in two different types. The first type of spectra, which will be subsequently referred to as having a *band* character, includes among others the KL_1V , $KL_{2,3}V$, and $L_{2,3}VV$ Auger spectra of magnesium and some of its compounds (*V* designates a valence-band level), the $L_1L_{2,3}V$ and $L_{2,3}VV$ spectra of silicon and the KVV spectrum of graphite. If one allows for some complications,

like the ones derived from the failure of the assumption of constant transition-matrix elements⁵ for all the states of the valence band, the above spectra have line shapes that can be directly correlated with the DOS, as determined by alternative techniques or by theory. In transitions involving two valence-band levels, there is also an additional problem of numerical deconvolution. It is likely that Auger spectra of other free-electron-like metals and semiconductors belong to this group too. On the other hand, there is a second type of spectra, which will be termed *quasi-atomic*, where this correlation between Auger line shape and DOS cannot be established. On the other hand, a multiplet structure arising from electrostatic two-hole interaction in the final state is present. In XVV transitions (*X* designating an inner level), instead of a line shape closely resembling a convolution of the density of states modulated by transition-matrix effects, one observes a series of sharp peaks, whose energies can be interpreted in terms of multiplet *atomic* configurations. These types of spectra have been found in previous investigations of two kinds of systems. One is the case of LVV and MVV spectra of metals with narrow *d* bands like copper, zinc, silver, and nickel.^{5,10-14} The other is given by Auger spectra of electronegative elements in the form of compounds like the KVV oxygen spectrum in oxide compounds.¹⁵ The Auger line shape of all these systems reflects the quasiatomic characteristics indicated above and, therefore, solid-state band effects are not apparent.

A unifying description of the above empirical results is obtained by making use of the concept of electron localization in a band. In fact, spec-

tra showing a band character are associated to a final state involving delocalized holes in quasi-free-electron bands. On the other hand, all the spectra having a quasiautomic character are connected with bands involving rather localized electrons. Another type of Auger transitions must be considered in connection with these ideas. These are the ones involving the neutralization of probe ions impinging on the surface in ion neutralization spectroscopy (INS).¹⁶ The question can then be put forward of why AES and INS, both of which leave the same double-hole final state in the metal atom, give such different results: a quasiautomic spectrum the first and a bandlike spectrum the second.

The above question is of great practical importance. This is so mainly because of the possibility of using AES as an alternative to INS in surface physics. This possibility was first explored by Sickafus⁶ for the system sulphur on nickel, for which INS data were also available. The obvious difference between the two techniques lies in the initial state, which in AES is localized in the *same* atom that is being probed, whereas in INS it is located at about an interatomic distance. Physically, one might conceive that the presence of this plus charge, in AES, strongly modifies the characteristics of the periodic potential giving rise to the band and tends to make the system more atomiclike. On the other hand, the INS process is an interatomic deexcitation and it is likely that the influence of the external probing charge is considerably screened in the metal. Following these ideas, a systematic investigation was started in our laboratory in order to clarify the origin of the observed AES line shape in adsorbate layers on transition metals, and particularly, the role of the localized hole in the initial state. In this connection, two types of deexcitation processes were identified in AES spectra of some adsorbates chemisorbed onto transition metals.¹⁷ These are, namely, normal Auger processes leading to quasiautomic spectra and a new kind of interatomic processes between adsorbate and substrate. The latter are in a way similar to INS transitions, with the adsorbate playing in AES a role similar to the probe ion in INS. In fact, interatomic Auger peaks were found to be related to the DOS of the substrate and little perturbed by the effects discussed before.

The purpose of the present paper is threefold. First, to present a set of systematic new data of the fine structure of adsorbate Auger peaks, covering a wide range of gas adsorbates on transition metals. These data are discussed in view of providing further supplementation to the idea of substrate-adsorbate interatomic transitions put forward earlier. Second, to provide a detailed

analysis of the intra-atomic part of the adsorbate spectra and of its quasiautomic character. Particular attention is paid to the determination of energy shifts, and to the estimation of relaxation contributions associated to final-state interactions. At present, the proper understanding of these shifts seems most relevant in view of the importance of such final-state effects not only in AES but also in other spectroscopies like photoemission.¹⁸ Finally, the paper examines critically the conditions under which a connection can be established between AES and DOS. The organization of the article is as follows: in Sec. II the experimental techniques are described and their limitations discussed. In Sec. III the experimental results are given; they are grouped into different headings corresponding to different adsorbates and a final subsection devoted to the empirical recompilation of the general trends common to all the systems studied. Section IV deals with the origin of the features in the line shapes of the spectra, the guideline of the discussion being the distinction between intratomic and interatomic processes. Section V is dedicated to the study of the role of localization in connection with the band versus quasiautomic behavior of the spectra and to the analysis of the conditions for which DOS and AES can be related. Finally, Sec. VI takes care of the main conclusions of this work.

II. EXPERIMENTAL

The experiments were performed in a commercial low-energy-electron-diffraction (LEED) Auger system, which operated in an ultrahigh vacuum in the range of 10^{-9} Torr. Copper targets were in the form of (100) and (110) single crystals whereas nickel and iron were polycrystalline ribbons. All three were mechanically polished, and copper subsequently electropolished, in a phosphoric acid solution, prior to their insertion into the vacuum chamber. Zinc targets were thin layers evaporated *in situ* onto silicon substrates. Final cleaning of the specimens was always carried out by ion bombardment followed by annealing.

Auger electron spectra were obtained by means of a standard cylindrical mirror analyzer, the coaxial electron gun operating at normal incidence. The energy resolution of our cylindrical mirror analyzer was of the order $\Delta E/E \sim 0.006$. This sets an upper limit to the resolvable fine structure of certain peaks, particularly oxygen, for which $\Delta E \sim 3$ eV. For this reason, we do not specify peak widths. Also, the very weak structure eventually appearing around the most definite peaks might well be invisible. The electron energies presented in this article were obtained by measuring the voltage applied to the outer cylinder of the cylindrical mirror analyzer (the inner one

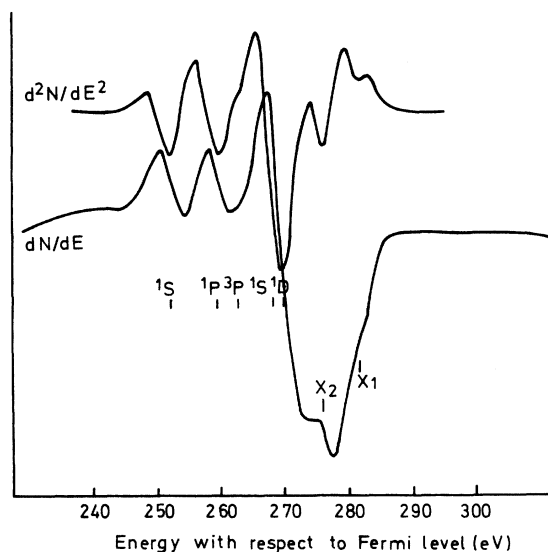


FIG. 1. KVV Auger spectrum of carbon on nickel is shown in the dN/dE and d^2N/dE^2 modes for the purpose of comparison. The spectral terms calculated as explained in the text are also shown. These are in order of increasing energy KL_1L_1 ($1S$), KL_1L_{23} ($1P$ and $3P$), $KL_{23}L_{23}$ ($1S$ and $1D$). The peaks, labeled X_1 and X_2 in the text, are also shown.

being grounded) and multiplying it by a factor depending on the geometrical configuration. This factor was determined experimentally by just measuring the ratio between the energy of the elastic peak and that of the incident beam. In this calibration procedure, the contact potential correction due to the slightly different work functions of the inner cylinder and the gun cathode was neglected. This is thought to introduce a maximum relative error of 0.1% in the Auger energies. The energies obtained by this procedure are, in fact, kinetic energies referred to the vacuum level of the inner cylinder, which is displaced with respect to the sample vacuum level by an amount equal to the difference between the work functions of the sample and of the inner cylinder. The work functions of the chemisorption systems studied in the present work are difficult to estimate and it is, then, better to refer the energies to the sample Fermi level by just adding to the energy referred above the work function of the inner cylinder. The latter is taken to be $\phi_c = 4.5$ eV. Throughout this article all our experimental Auger energies will be referred to the sample Fermi level.

Some of the spectra are shown in a double derivative mode d^2N/dE^2 , $N(E)$ being the secondary electron spectrum. This is easily done by tuning the lock-in amplifier to the second-harmonic component of the modulated signal. Provided small peak-to-peak modulations are used, this method allows a more accurate measurement of fine-

structure peaks (it is easier to place a minimum than an inflection point) and also a better elimination of the background. For the purpose of comparison, Fig. 1 shows the KLL Auger spectrum of carbon on nickel in both the usual dN/dE and the d^2N/dE^2 modes.

We briefly describe now the procedures used for adsorption on the metal substrates. A carbon chemisorbed layer on nickel was obtained by exposure to a carbon monoxide atmosphere and subsequent elimination of oxygen by heating. The adsorption of oxygen was accomplished by exposure to an O_2 atmosphere. An exposure of 1 langmuir ($1L = 10^{-6}$ Torr sec) on nickel was already detectable. For Cu(110) a 10-L exposure showed a (2×1) LEED structure which led to a $c(6 \times 2)$ structure when increasing the exposure. In Cu(100) a $c(2 \times 2)$ structure was obtained. Chlorine adsorption was obtained by thermal decomposition of $AlCl_3$ in the chamber. An exposure of 10 L on Cu(100) resulted in the apparition of a sharp $c(2 \times 2)$ LEED structure. All of these exposures were obtained keeping the sample at room temperature. Nitrogen was adsorbed through ion bombardment in a residual nitrogen atmosphere. In the (110) face, the observed structure was (3×2) ; In the (100) face, $c(2 \times 2)$. Sulphur was diffused from the bulk to the surface by thermal annealing. In both copper faces, this resulted in the apparition of complex ordered structures.

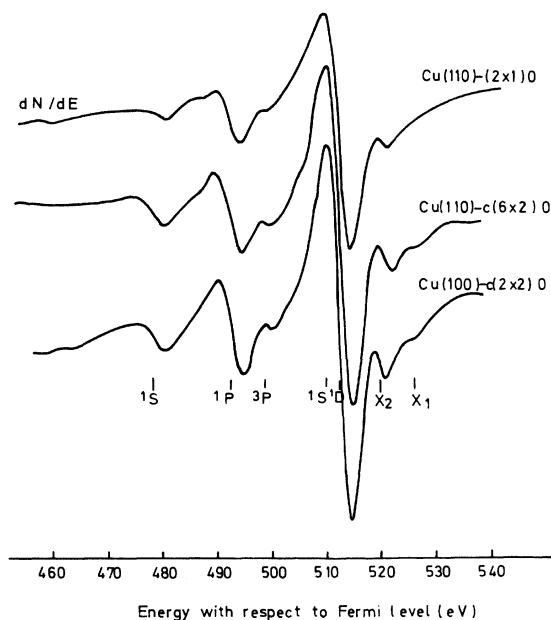


FIG. 2. KVV Auger spectrum of several surface structures of oxygen chemisorbed on copper. See Fig. 1 caption.

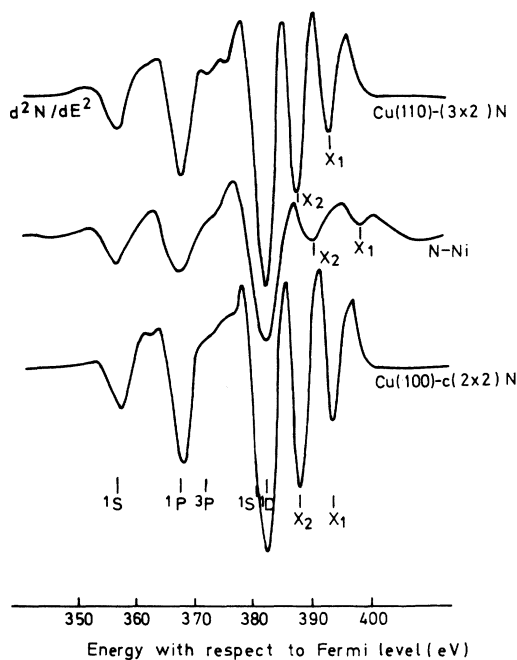


FIG. 3. KVV Auger spectrum of nitrogen adsorbed on copper and nickel. See Fig. 1 caption.

III. RESULTS

A. Presentation of results

In this section, we present results concerning the KVV or $L_{23}VV$ Auger spectra of adsorbate atoms in eleven combinations of carbon, oxygen, nitrogen, sulphur, and chlorine adsorbates on copper, nickel, iron, and zinc substrates. The valence band of these systems include contributions from the conduction band of the substrate and from s and p levels of the adsorbate.

The observed line shapes are shown in Figs. 1-6. A short report of these results has been pub-

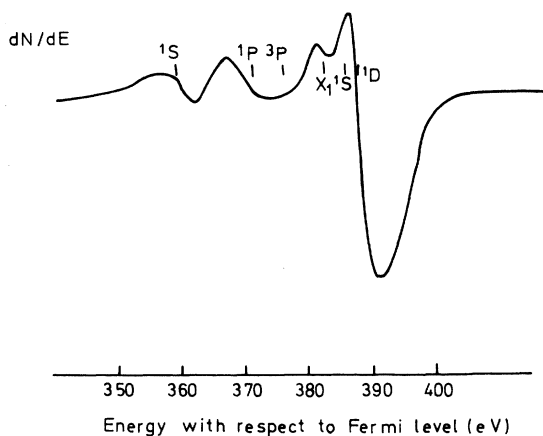


FIG. 4. KVV Auger spectrum of nitrogen on zinc. See Fig. 1 caption.

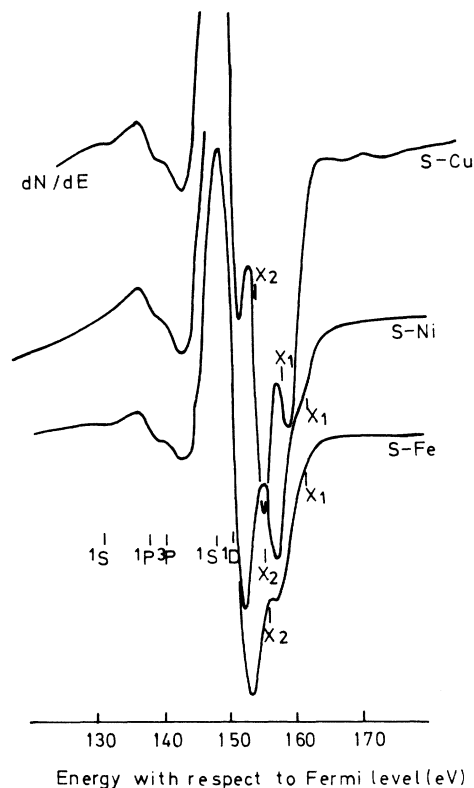


FIG. 5. $L_{23}VV$ Auger spectrum of sulphur adsorbed on copper, nickel, and iron. See Fig. 1 caption.



FIG. 6. $L_{23}VV$ Auger spectrum of chlorine adsorbed on Cu(100) in the dN/dE mode. See Fig. 1 caption.

TABLE I. Carbon.

System	C-Ni	CH ₄ ^{a,d}	CO-Mo ^{b,e}	C-Ni ^{c-e}	Calculated C-Ni
	282.5				
	276		275		
Peak	269.5	250.0	272	270	269.5 <i>KL₂₃L₂₃</i> (¹ D)
energies					268.4 <i>KL₂₃L₂₃</i> (¹ S)
in eV		243.3			262.8 <i>KL₁L₂₃</i> (³ P)
	260	237.0	262	257	259.6 <i>KL₁L₂₃</i> (¹ P)
	252.5	229.4	254	249	252.5 <i>KL₁L₁</i> (¹ S)

^aReference 38.^bJ. T. Grant and T. W. Haas, Appl. Phys. Lett. **16**, 172 (1970).^cJ. P. Coad and J. C. Rivière, Surf. Sci. **25**, 609 (1971)^dReferred to the vacuum level.^eEnergy measured at the minimum in the *dN/dE* mode.

TABLE II. Oxygen.

System	O-Ni	O-Cu	O-Cu (111) ^{a,d,e}	H ₂ O ^{b,d}	O-Ni ^{c-e}	Calculated O-Cu
		525.9				
	521	520.7	519			
				500.5		
	511.5	512.5	513	498.6	516	512.5 <i>KL₂₃L₂₃</i> (¹ D)
				493.8		510.2 <i>KL₂₃L₂₃</i> (¹ S)
Peak	503	505		486.8		
energies	499.0	500.2	498	482.2		498.9 <i>KL₁L₂₃</i> (³ P)
in eV	492.6	492.9	492	474.6	495.2	492.5 <i>KL₁L₂₃</i> (¹ P)
	487.5	489		469.2		
		485				
	477.9	478.2	477	457.4	480.6	478.2 <i>KL₁L₁</i> (¹ S)
	472	474		448		

^aL. H. Jenkins and M. F. Chung, Surf. Sci. **26**, 151 (1971).^bReference 24.^cA. M. Horgan and I. Dalins, Surf. Sci. **36**, 526 (1973).^dSee footnote Table I.^eSee footnote Table I.

TABLE III. Nitrogen.

System	N-Cu	N-Ni	N-Zn	Mo ₂ N ^a	NH ₃ ^{a,c}	N-Ni ^{b,c}	Calculated N-Cu
	393.9	398.0	381.0				
	388.4	390.8		392.0		387	
	382.8	382.8	386.3	385.0	382.2	378	382.8 <i>KL₂₃L₂₃</i> (¹ D)
Peak							381.2 <i>KL₂₃L₂₃</i> (¹ S)
energies	376.6				377.4		
in eV	373.2	374.5	375.8	375.0			373.1 <i>KL₁L₂₃</i> (³ P)
	368.8	368.5	368.5	372.0	369.6	364	368.5 <i>KL₁L₂₃</i> (¹ P)
	358.2	357.5	358.5	358.9	361.6	352	358.2 <i>KL₁L₁</i> (¹ S)

^aReference 28.^bE. N. Sickafus and F. Steinrisser, J. Vac. Sci. Technol. **10**, 43 (1973).^cSee footnote (d) Table I.

TABLE IV. Sulphur.

System	S-Cu	S-Ni	S-Fe	S-Ni ^{a,c}	S-Ni ^{b,c}	Calculated S-Cu
	159.1	161.3	162.4	158	157.3	
	154.7	156.9	157.0	153	153.8	
	150.8	151.3	150.9	147	148.5	150.8 $L_{23}M_{23}M_{23}$ (³ P, ¹ D)
Peak	147.5					148.5 $L_{23}M_{23}M_{23}$ (¹ S)
energies	146.3					
in eV	142.2	142.7	142.3	139		141.1 $L_{23}M_1M_{23}$ (³ P)
	138.4	138.9	138.0	134		138.6 $L_{23}M_1M_{23}$ (¹ P)
	131.8	131.4	130.5			131.8 $L_{23}M_1M_1$ (¹ S)

^aReference 6.

^bJ. P. Coad and J. C. Rivière, Proc. R. Soc. Lond. A **331**, 403 (1972).

^cSee footnote (d) Table I.

lished earlier.¹⁷ The measured energies of the peaks appearing in the fine structure of these spectra are summarized in Tables I–V. A different table is provided for each adsorbate. These tables include also, when available, results of other authors for the same or comparable systems. When comparing these results, one has to have in mind two points: (i) Some authors measure their energies at the minimum of their peaks in the dN/dE mode; and (ii) energies are often referred to the vacuum level whereas we prefer using the Fermi level as a reference for the reasons pointed out in Sec. II. These circumstances are specified in the tables. Spectra of some gas molecules containing the adsorbate atoms as a component are also included. The last column (labeled “calculated”) is added in order to help to interpret a part of the adsorbate spectra. It includes data that are obtained by taking the experimental spectral terms associated to the corresponding Auger transition in the nearest rare gas (KLL in neon,¹⁹ $L_{23}MM$ in argon²⁰) and scaling them as follows: the energy scale of the rare-gas Auger spectrum is linearly contracted in order to make the lowest- and highest-energy peaks of the rare-gas spectrum coincident, respectively, with the lowest-energy and main peak (most intense one) of the adsorbate spectrum. In the case of neon, these lowest- and highest-energy peaks correspond to the KL_1L_1 (¹S) and $KL_{23}L_{23}$ (¹D) spectral terms. For argon, they are taken as the $L_{23}M_1M_1$ (¹S) and the average of the $L_{23}M_{23}M_{23}$ (¹D) and (³P). The adsorbate peaks associated to the three $L_{23}M_{23}M_{23}$ rare-gas spectral terms are not resolved. However, when scaling, as described, only the ¹D and ³P terms of the gas are averaged on the basis of a relative intensity argument. Spectral term positions, according to the previous discussion, are also shown in the Figs. 1–6.

B. General trends of adsorbate Auger spectra

In this subsection, some general trends concerning the behavior of the line shapes of the ad-

sorbate Auger spectra are given. These trends can be derived from inspection of Figs. 1–6 and from Tables I–V.

(i) For all the substrate-adsorbate systems studied in this investigation, there is a part of the spectrum consisting in a series of peaks appearing, except for N-Zn, at the low-energy side of the main peak (including the latter) whose relative energies are insensitive within $\sim \pm 1$ eV to the nature of the substrate. This may be inferred from Tables II–IV. We shall term this part of the spectrum as the adsorbate contribution. Also, under the present conditions of resolution, the corresponding line shapes show little changes for the different substrates, as can be seen in Figs. 3 and 5.

(ii) The rest of the spectrum, consisting generally of two peaks on the high-energy side of the main peak, depends on the nature of the substrate and will be referred to as the substrate contribution. For a given adsorbate, these peaks called X_1 and X_2 appear at decreasing kinetic energies in the succession nickel or iron, copper, and zinc substrates. In the case of zinc, the peak X_1 has a kinetic energy even smaller than that of the main peak and, consequently, appears on the low-energy side of the latter. In this case, it seems that the peak X_2 is not visible (Fig. 4).

The relative energy of peak X_1 , with respect to the ionization energy corresponding to the core level involved in the Auger transition, is practical-

TABLE V. Chlorine.

System	Cl-Cu	Cl-Ni	Calculated Cl-Cu
	195.9	198.5	
	192.4	192.5	
	191.1		
Peak	184.9	184.5	184.9 $L_{23}M_{23}M_{23}$ (³ P, ¹ D)
energies	182.0	181.2	182.6 $L_{23}M_{23}M_{23}$ (¹ S)
in eV	179.2	178.5	
	174.5	174.0	175.2 $L_{23}M_1M_{23}$ (³ P)
	171.4	170.5	172.7 $L_{23}M_1M_{23}$ (¹ P)
	165.9	166.9	165.9 $L_{23}M_1M_1$ (¹ S)

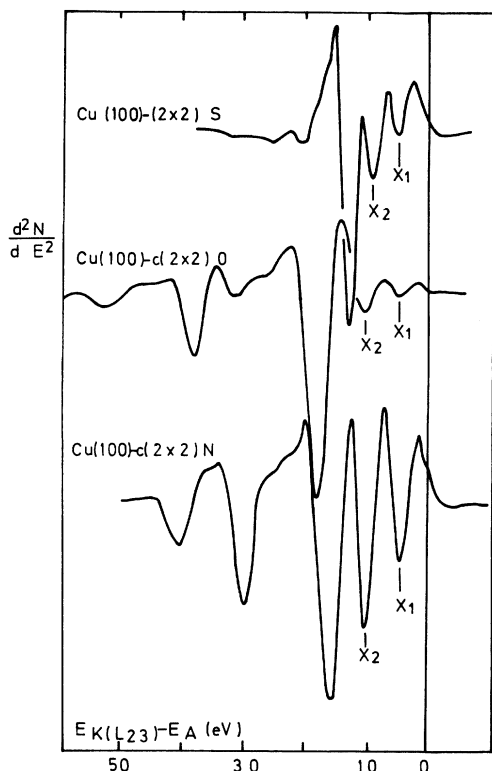


FIG. 7. Second-derivative spectra of the Auger peaks of S, O, and N adsorbed on a Cu(100) crystal. The vertical full line corresponds to the point of the spectra where energy equals the binding energy of the inner level of the corresponding Auger transition.

ly the same for all the adsorbates on the same substrate (Table VI). This point is illustrated in Fig. 7. In this figure, the energy scale represents binding energies of two holes in the final state of the system referred to the Fermi level. The latter, taken as the zero energy in the figure, is associated to an Auger transition leaving two holes at the Fermi level, the corresponding Auger electrons having an energy equal to the binding energy of the core hole.

(iii) The intensity of peaks X_1 and X_2 , for a given substrate, depends on the nature of the adsorbate. The more intense peaks correspond to nitrogen and sulphur adsorbates and the weaker ones to oxygen and chlorine.

(iv) The intensity and position of peaks X_1 and X_2 relative to the main peak do not depend either on the substrate orientation or on the adsorbate layer crystal structure for the case of adsorbates on copper (other metal substrates were in polycrystalline form).

IV. LINE SHAPE OF AUGER ADSORBATE SPECTRA

A. Quasiatomic versus band Auger spectra

Auger electron spectra in gases are now well understood. The intermediate coupling theory of

Asaad and Burhop²¹ was recently improved by Shirley,²² taking into account a previously neglected intra-atomic relaxation effect, and calculations along these lines are in very good agreement with experiments. The fine structure of Auger spectra associated to $ijkl$ transitions (j initial hole state, k and l final hole states) is found to consist in a series of rather narrow peaks, which can be labeled by an index Y . If their corresponding energies are written

$$E_{at}(ijkl, Y) = E_{at}(j) - E_{at}(k) - E_{at}(l) - \Delta E_{at}(kl, Y), \quad (1)$$

where $E_{at}(i)$, $i = j, k, l$, is the binding energy of level i in the atom as measured, for example, by x-ray photoemission spectroscopy (XPS), the energy shift ΔE can be written according to the above-mentioned theory and keeping the notations of Ref. 22:

$$\Delta E_{at}(kl, Y) = \mathcal{F}(kl, Y) - R_a(kl). \quad (2)$$

Here, the first term \mathcal{F} is due to static interaction between the two holes in the final state. The index Y refers to the spectral term of the corresponding final-state configuration. When more than a spectral term is possible, several peaks appear in the spectrum. The R_a term is called intra-atomic relaxation. Physically, it takes into account the fact that a relaxation of the outer atomic levels occurs around the k hole and, consequently, the interaction energy between the k

TABLE VI. Binding energies of electron levels responsible for X_1 peak in Auger spectra.

Adsorbate and observed LEED structure	Energy of peak X_1^a (eV)	$E(j)$ (eV)	$\frac{1}{2}[E(j) - E(X_1)]$ (eV)
Cu(100) - c(2x2)N	393.9	399.0 ^b	2.5
Cu(100) - (2x2)S	159.1	164.0 ^c	2.5
Cu(100) - c(2x2)O	525.9	531.2 ^d	2.7
C-Ni	282.5	283.8 ^f	0.7
N-Ni	398.0	399.0 ^b	0.5
S-Ni	161.3	164.0 ^c	1.3
S-Fe	162.4	163.2 ^e	0.4
N-Zn	381.0	399.0 ^b	9.0

^a See Tables I-V.

^b From data of nitrogen compounds, D. N. Hendrickson, J. M. Hollander, and W. J. Jolly, *Inorg. Chem.* **8**, 2642 (1969); and P. Finn, R. K. Pearson, J. M. Hollander, and W. J. Jolly, *ibid.* **10**, 378 (1971).

^c From data of chemisorbed sulphur on nickel, J. P. Coad and J. C. Rivière, *Proc. R. Soc. Lond. A* **331**, 403 (1972).

^d Averaging data from S. Evans, E. L. Evans, D. E. Parry, M. J. Tricker, M. J. Walters and J. M. Thomas, *J. Chem. Soc. Faraday Disc.* **58**, 97 (1974); and T. Robert, M. Bartel, and G. Offergeld, *Surf. Sci.* **33**, 123 (1972).

^e From data of the bulk compound, H. Binder, *Z. Naturforsch. A* **28b**, 255 (1973).

^f From J. A. Bearden and A. F. Burr, *Revs. Mod. Phys.* **39**, 125 (1967).

and l holes in the final state is somehow reduced.

On the other hand, Auger spectra in solids are much more complicated and a simple description in terms of formulas like (1) is not possible in general. However, most of the solid materials studied so far show a behavior that falls near one of the two limits described in the following.

The *quasiatomic* limit refers to systems, with Auger spectra, whose fine structure is not very different from the one found in atomic spectra. Typical examples are Auger spectra of transitions involving only core levels. This behavior is also met in spectra involving valence bands in transition metals with d bands^{5,10-14} and in spectra of electronegative elements of certain compounds like MgO.¹⁵ The fine structure of these spectra includes spectral terms associated to final-state configurations in the corresponding atom (or ion). The energy of the peaks related to these spectral terms can be calculated by an extension of Eqs. (1) and (2)

$$E(jkl, Y) = E(j) - E(k) - E(l) - \Delta E(kl, Y), \quad (3)$$

$$\Delta E(kl, Y) = \mathcal{F}(kl, Y) - R_a(kl) - R_e(kl), \quad (4)$$

where the subscripts "at" have been dropped to indicate that all energies correspond now to the solid. In the expression of the energy shift ΔE , there is a new term R_e called extra-atomic relaxation energy. Physically this term accounts for the partial screening of one of the two final-state holes by the Fermi electron gas. Evaluations of $^{10}R_e$ are in reasonably good accord with experiments. It is also worth remarking that peak widths in quasiatomic spectra are comparable to those in gas atoms.

The *band* limit refers to those transitions involving the V valence band, in which the band structure of the solid is apparent. Some examples of these are the KL_1V , $KL_{23}V$, and $L_{23}VV$ transitions of magnesium and some of its compounds,⁷ the $L_1L_{23}V$ and $L_{23}VV$ transition of silicon and the KVV transition of graphite.² It seems likely that this behavior is also typical of most quasi-free-electron elements and compounds. Instead of a succession of rather narrow peaks, corresponding to spectral terms, these spectra show a much broader structure, whose features are related to the density of states of the band. If one assumes constant matrix elements among the different states in the valence band, the electron signal $N(E)$, as a function of kinetic energy E referred to the Fermi level, can be written

$$N(E) \propto \mathcal{D}[E(j) - E(k) - E] \quad (5)$$

for transitions involving one final hole l in the valence band, or in terms of ϵ , the band energy measured down into the band from the Fermi level

$$\epsilon \equiv \frac{1}{2}[E(j) - E],$$

$$N(E) \propto \int_0^{\epsilon'} \mathcal{D}(\epsilon - \Delta) \mathcal{D}(\epsilon + \Delta) d\Delta, \quad (6)$$

$$\epsilon' \begin{cases} = \epsilon, & 0 \leq \epsilon \leq \frac{1}{2}E_F, \\ = E_F - \epsilon, & \frac{1}{2}E_F \leq \epsilon \leq E_F, \end{cases}$$

for transitions involving two final holes in the valence band, where $\mathcal{D}(\epsilon)$ is the valence-band density of states and E_F is the Fermi energy. In both cases there is no energy shift equivalent to ΔE in Eq. (3). Notice that Eq. (3) can be obtained from (5) or (6) by substituting a δ function for the band density of states and adding a shift ΔE .

In short, previous investigations seem to suggest that AES spectra involving the valence band are of quasiatomic character for d -band transition metals and for electronegative atoms in insulator compounds, but are of band character for quasi-free-electron metals and semiconductors. These limits seem to correspond physically to localized and delocalized electrons in the final state. It has been suggested^{10,11} that localization of valence electrons leads to atomiclike Auger spectra. An earlier argument points out¹⁴ that an electron in a band can be considered to be localized, as far as Auger deexcitation is concerned, when the width of the band is small compared to the width of the level in which the initial hole is located. This is, in fact, the case in the systems showing a quasiatomic behavior, that have been indicated before. In the following, we investigate the situation in the case of adsorbed layers.

B. Model for adsorbate core hole deexcitation

In this section a model for the deexcitation of a core hole in an adsorbed atom onto a transition metal is discussed. This model has been previously proposed¹⁷ by two of the present authors. Here, a more complete experimental evidence is provided and a thorough discussion of the implications of the model presented.

The ideas later discussed are based on certain physical similarities between AES and the ion neutralization technique (INS) first developed by Hagstrum.¹⁶ In short, INS samples the valence band of, say, a transition metal by analyzing the Auger spectrum arising from the neutralization of an inert-gas ion impinging on the metal surface. As the binding energy of the hole in the gas ion is not very large (~ 10 – 20 eV), only Auger transitions involving two holes from the metal valence band in the final state are allowed. Deconvolution of Eq. (5) is, then, required. The important point is that the density of states of the transition metal does not seem to be perturbed by the presence of the gas atom hole and, in fact, bandlike Auger spectra are obtained in nickel and copper.²³ This is very different from the behavior that is

observed in AES of transition metals (see Sec. IV A), in which quasiatomic spectra, not related to their band characteristics, are obtained. The main difference between AES and INS lies in the localization of the initial-state hole. It seems that if this hole is localized in the same atom of the two final state holes, the perturbation of the band is important (*intra-atomic* deexcitation), but when it is in a different atom (*interatomic* deexcitation), as in INS, the perturbation effects are minimized.

Our model considers the deexcitation of a core hole in an adsorbate atom as a competitive process between transitions involving electrons in the valence band of the metal (interatomic) and those involving electrons in the upper electron levels of the adsorbate atom itself (intra-atomic). The former are INS-like, the main difference being the binding energy of the probing hole, that is of the order of 10–20 eV in INS but can be as much as ~500 eV in chemisorbed oxygen. Intra-atomic transitions have no counterpart in INS due to the fact that in the latter the initial state hole is in the uppermost level. On the basis of the previous discussion, it is expected that the interatomic contribution to the spectrum reflects the density of states of the metal band, i. e., is of a band character. On the other hand, the intra-atomic contribution arises from processes in which the localization of the adsorbate upper electron levels onto the initial-state core hole is associated to strong perturbation of the corresponding levels. This gives rise to a contribution to the spectrum of a quasiatomic character which is not directly related to the adsorbate levels in the band. On the grounds of simple arguments based on transition-matrix elements, it is also expected that the intra-atomic part of the spectrum is usually going to be dominant.

This model is based on the comparative behavior of the adsorbate peaks in the series of metal-adsorbate systems described in Sec. III B. We argue that the adsorbate-dependent low-energy region of the spectrum described there is due to intra-atomic transitions in the adsorbate. The strong perturbation of the upper levels due to the localization of the initial inner hole causes the appearance of quasiatomic spectra with spectral terms that depend on final-state configuration and, therefore, are mainly controlled by the nature of the adsorbate. Slight differences in position and different intensities for the various substrates might be thought of in terms of bonding alterations when passing from one couple to another. Moreover, their energies can be explained in terms of spectral terms associated to final-state hole-hole interactions (Sec. III). We propose that the substrate-dependent high-energy side of the spectrum

is due to interatomic transitions from the metal valence band. Among these transitions, those originated from the *d* component of the band are the most distinct and, in fact, dominate the picture. This behavior is also characteristic of *XVV* spectra in the pure metal, in which spectral terms from *d*-band holes are the main cause of structure.^{10–14} The peak indexed X_1 would, then, result from deexcitations of the adsorbate hole from electrons in the metal *d* band and emission of the same type of electrons. This idea is strongly supported by the comparison of the apparent binding energies of the electrons contributing to X_1 (4th column in Table VI) with *d*-band binding energies of the substrate metal E_d . It is clear that the correlation is very good. The case of zinc is particularly interesting, as the large depth of its *d* band (~10 eV) makes it possible that adsorbate levels have much lower binding energies. Consequently, the interatomic peak X_1 appears, in this case, at the low-energy side of the main peak, as observed. These observations can be written in the form

$$\frac{1}{2}[E_{X_1} - E(j)] = E_d. \quad (7)$$

In the following, we develop the model in a separate discussion of the fine structure associated to interatomic and intra-atomic transitions in the light of the proposed model.

C. Interatomic transitions

The peak X_1 in the adsorbate spectrum has been interpreted, in Sec. IV B, as arising from the deexcitation of an adsorbate hole with binding energy $E(j)$ by electrons from the *d* band of the substrate metal. It is worth noticing that Eq. (7) is equivalent to Eq. (3), by substituting E_d for $E(k)$ and $E(l)$ and making $\Delta E = 0$. The latter point is very important as it shows that these interatomic peaks reflect an unperturbed band structure and are, then, closely related to INS spectra.

It is also enlightening to compare the Auger spectra of oxygen on an adsorbate metal with the corresponding spectrum in a molecule of comparable ionicity (as estimated from electronegativity differences). Figure 8 shows the Auger spectrum of oxygen adsorbed on copper and the one of oxygen in a water molecule.²⁴ It is clear that the peaks in the low-energy side are related in both structures. On the other hand, the two peaks in the high-energy side of oxygen on copper (interatomic according to our model) are not at all visible in the water spectrum. This observation is in very good agreement with our proposed mechanism of a double contribution to the Auger line shape.

Auger transitions involving a mechanism similar to the one described as *interatomic* here have

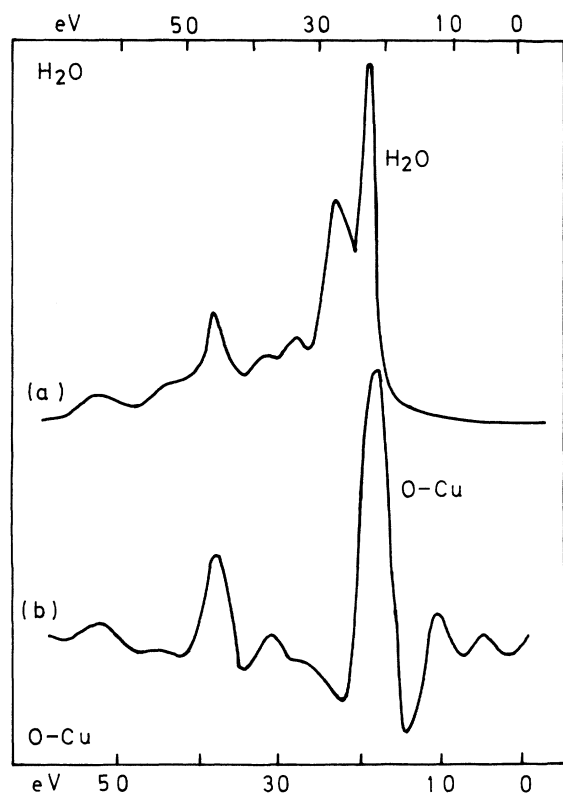


FIG. 8. *KLL* oxygen Auger peak in H_2O (curve a) and chemisorbed on Cu (curve b). Curve a has been taken from Ref. 26. Curve b is presented in the $-d^2N/dE^2$ mode.

been recognized by other authors in experiments on lithium fluoride,²⁵ magnesium oxide,²⁶ and magnesium fluoride²⁷ and in ammonia adsorbed on molybdenum.²⁸ Also, linewidth measurements in photoemission²⁹ seem to support the existence of interatomic deexcitations. Besides, interatomic peaks arising from deexcitations of core holes in transition-metal atoms from electrons of the *d* band localized on neighbors in the crystal structure have also been tentatively identified in *MVV* Auger spectra of copper and nickel.¹⁴ It is worth remarking that these peaks have $\Delta E = 0$, in contrast to the peaks of the "normal" (intra-atomic) Auger transitions, which are controlled by final-state spectral terms structure. Magnesium oxide provides also a good answer to the question of whether interatomic transitions can ever become dominant. A previous investigation of the present authors¹⁵ has indeed shown that the $L_{23}VV$ magnesium peak in magnesium oxide arises, in fact, from an interatomic transition. Magnesium oxide is a rather ionic compound and, consequently, a hole in an inner *L* level finds no electron in upper levels localized on the magnesium ion. Therefore, there are no competitive deexcitation processes because only interatomic transitions from electrons

localized near the oxygen ion are possible. Deconvolution of the magnesium peak in the compound shows an encouraging agreement with the density of states of the compound. On the other hand, the fine structure of the oxygen Auger spectrum in that compound can be explained in terms of multiplet splitting in the final two-hole state of the oxygen ion.

It is clear that the term "interatomic" is an oversimplification used to describe a much more complex situation. When a gas atom is adsorbed on a surface, the tails of the wave functions of the electrons in the metal-band tunnel into the region of the adsorbed atom and, consequently, there is, on the latter, a certain electron density at the corresponding energy. It is, then, better to think of interatomic processes in terms of tunnelling. Among the different systems investigated in the present work, the intensity of the interatomic part of the spectrum, with respect to the main intra-atomic peak, is large for nitrogen and sulphur adsorbates whereas it is rather small for oxygen and chlorine. Even if no conclusive remarks can yet be made, the results go in the sense that interatomic peaks decrease in intensity as the ionicity of the bond increases.

In order to qualitatively check whether INS and interatomic AES involve comparable tunnelling, the yield of both processes per initial available hole has been compared in both techniques. The number of electrons associated to deexcitations involving twice the substrate *d* band per incident ion and per electronvolt may be directly drawn from INS data.¹⁶ Its value is 15×10^{-3} for ions incident on pure nickel surfaces and 5×10^{-3} for nickel surfaces with a chemisorbed sulphur layer. This is reasonably compared with the figure of 8×10^{-3} that we derive from our AES data by obtaining the ratio between the intensity of our peak X_1 and the total number of initial holes given by the integral under the whole Auger line of $N(E)$.

Most of the previous discussion about interatomic transitions has dealt with one of the peaks of the adsorbate spectrum (the most energetic one except for zinc substrates). However, there is a second peak which seems also to be connected with interatomic transitions. This peak labeled X_2 in the figures is found very often at an energy roughly halfway between peak X_1 and the main peak. It might be due to deexcitations involving one electron in the metal *d* band and another at the gas atom, in which case its energy shift ΔE would not be zero. However, an unambiguous interpretation of that peak has not yet been obtained.

D. Intra-atomic transitions

In Sec. IVB we have given the arguments leading to the identification of intra-atomic transi-

tion in Auger adsorbate spectra. In the present one, we discuss the implications of this idea. First, we examine the possible connections between the intra-atomic part of the Auger spectrum and chemical environment and, then, we make a careful analysis of relaxation effects associated to final-state configurations.

In Sec. III it was shown how the relative positions of the different peaks associated to a given adsorbate spectrum could be correlated to the spectral term of the nearest rare-gas atom. A similar scaling procedure has been shown³⁰ to provide a good correspondence between the Auger spectra of hydrofluoric acid molecules and neon atoms. We want to stress that the correspondence between adsorbate and rare-gas spectra is best for oxygen adsorbates. In this case, the correlation in the position of the fine-structure peaks, shown in Tables I–V, has been complemented by a comparison of the corresponding intensities. The agreement is good, the difference in relative intensities being less than 10%. We have also compared the Auger spectra of adsorbate atoms to those of simple molecules containing the same atoms. Whereas a good correlation has been found between the spectral terms of gaseous water and those of oxygen chemisorbed on copper (see Fig. 8 and Table II), no such correlation can be established in the case of rather covalent molecules like NO, CO, or O₂.²⁴ Also, there is a good correlation between the spectral terms of methane and those of carbon on nickel (Table I). These similarities in Auger spectra imply similar final two-hole configurations. Consequently, it seems to suggest, also, that the chemical state of the adsorbate atom is not very different from the corresponding state in the molecule. These results have implications in connection with the concept of surface molecule³¹ and, therefore, the correlations described above seem to encourage further work along these lines. For this purpose, an improvement in analyzer resolution would probably be extremely advantageous.

Intra-atomic transitions have been shown to arise from perturbed electron levels. The magnitude of such perturbation may be measured by its associated energy shift ΔE . The latter can be calculated by using Eq. (3). We take $E(jkl, Y)$ from our own data, and the binding energies of the involved levels from other authors. It is worth remarking that, in order to be precise, binding energies corresponding to the same systems, i.e., chemisorbed layers of the same gas on the same substrate should be used. This is possible, unfortunately, for only a few systems of the 11 that are presented in this paper. In order to have, at least, estimations for some of the other systems, we have used the binding-energy values of the cor-

responding bulk compounds, for example iron sulfide for the system sulphur chemisorbed on iron. This is probably a fair approximation for core levels in the initial state, i.e., for $E(j)$ values. For most of the systems studied here, this procedure amounts to doubling the number of gas-metal bonds. Appearance potential spectroscopy (APS) data in several transition metals³² seem to indicate that the maximum shift in an inner level for a surface atom with respect to a bulk one does not exceed ~ 1 eV. Direct comparison of x-ray photoemission spectroscopy (XPS) data for the chemisorbed layer and the compound, when both are available, confirm this physical idea. The situation concerning the outer chemisorbed levels, $E(k)$ and $E(l)$, is much more dubious. We have compared INS binding energies of $3p$ sulphur levels³³ for sulphur chemisorbed on nickel ($E = 4.6$ eV) with the corresponding mean values of $3p$ sulphur bands³⁴ in the bulk compound nickel sulfide ($E = 4.2$ eV). For this system, the substitution of the compound for the chemisorption values seems then reasonable. On the other hand, other systems, for which the comparison is possible, like nickel oxide, show large discrepancies. Oxygen chemisorbed on nickel has been studied by INS,³³ uv photoelectron spectroscopy³⁵ (UPS), and electron-loss spectroscopy³⁶ (ELS). A binding-energy value around $E_B = 5.5$ eV has been consistently found. Contrary to that, XPS measurements in the bulk compound³⁴ do not show any structure that can be related to an electron density of states around those values.

The results for ΔE , along with the photoemission data involved in the calculations, are given in Table VII. According to the above discussion, ΔE values, as those for sulphur on iron, which are calculated by using binding energies of p levels of the compound should be taken only as indicative. On the other hand, binding energies of the deeper s levels are more likely to be similar in the chemisorbed layer and in the bulk compound. The maximum error involved is thought to be under ± 1.0 eV in sp transitions and ± 2.0 in ss ones. The error in ΔE for pp transitions, in which all data correspond to chemisorbed layers, is probably under ± 0.5 eV and mainly related to the limitations of the detector.

Further insight into the microscopic relaxation mechanisms associated to Auger transitions can be gained if the extra-atomic relaxation energy R_e can be estimated from the above data. From the ΔE values of Table VII, one can obtain R_e from Eq. (4), provided $\mathcal{F} - R_a$ can be evaluated. This is difficult to do in practice because it is not clear which values of \mathcal{F} and R_a should be used. They are not the ones corresponding to the free adsorbate atom because the adsorbed atom electron

TABLE VII. Energy shifts and relaxation energies of several Auger adsorbate peaks. All energies in the table are in eV units.

System	Transition		Auger energy ^a	Binding energies				$\mathcal{F} - R_a^g$	R_e^f	Ionicity (%) ^g
	Levels	Spectral term		$E(j)^b$	$E(k)^c$	$E(l)^c$	ΔE^d			
O-Ni	$KL_{23}L_{23}$	1D	513.1	529.5	5.5	5.5	5.4	15.9	10.2 ± 1.5	51
	KL_1L_{23}	3P	497.9	529.5	5.5	21.5 ^h	4.6	12.8		
	KL_1L_{23}	1P	492.7	529.5	5.5	21.5 ^h	9.8	20.2		
	KL_1L_1	1S	478.5	529.5	21.5 ^h	21.5 ^h	8.0	17.8		
O-Cu	$KL_{23}L_{23}$	1D	513.2	531.2	5.9	5.9	6.2	15.9	9.4 ± 0.9	47
	KL_1L_{23}	3P	500.5	531.2	5.9	21.5 ^h	3.3	12.8		
	KL_1L_{23}	1P	493.4	531.2	5.9	21.5 ^h	10.4	20.2		
	KL_1L_1	1S	479.2	531.2	21.5 ^h	21.5 ^h	9.0	17.8		
S-Ni	$L_{23}M_{23}M_{23}$	$^1D^3P$	151.5	164.0	4.6	4.6	3.3	(10.0)	(6.7)	12
	$L_{23}M_1M_{23}$	3P	143.4	164.0	4.6	14.2 ^h	1.8			
	$L_{23}M_1M_{23}$	1P	139.0	164.0	4.6	14.2 ^h	6.2			
	$L_{23}M_1M_1$	1S	130.9	164.0	14.2 ^h	14.2 ^h	4.7			
S-Fe	$L_{23}M_{23}M_{23}$	$^1D^3P$	150.9	163.2	4.0 ^h	4.0 ^h	4.3 ⁱ	(10.0)	(5.7)	12
	$L_{23}M_1M_{23}$	3P	142.3	163.2	4.0 ^h	14.0 ^h	2.9 ⁱ			
	$L_{23}M_1M_{23}$	1P	138.0	163.2	4.0 ^h	14.0 ^h	7.2 ⁱ			
	$L_{23}M_1M_1$	1S	130.5	163.2	14.0 ^h	14.0 ^h	4.7 ⁱ			

^a See data Tables I-V.

^b XPS photoemission data: O-Ni, C. R. Brundle and A. F. Carley, Chem. Phys. Lett. **31**, 423 (1975); O-Cu, S-Ni, and S-Fe see footnotes c, d, and e of Table VI.

^c O-Ni: Data of L_{23} from INS (Ref. 33), UPS (Ref. 35), and ELS (Ref. 36), L_1 data from bulk values of NiO (Ref. 34). O-Cu, L_{23} data from S. Evans *et al.* (see footnote d Table VI); L_1 data as for O-Ni. S-Ni: L_{23} data from INS (Ref. 33) or ELS (Ref. 39), L_1 data from the bulk compound (Ref. 34). All S-Fe data from bulk values of A. Ohsawa, H. Yamamoto, and H. Watanabe, J. Phys. Soc. Jpn. **37**, 568 (1974).

^d From Eq. (3).

^e H_2O ΔE values from Auger (Ref. 24) and binding energies from XPS (Ref. 37) as explained in the text. HF values from Ref. 30.

^f Values in brackets are only indicative (see text).

^g As estimated from electronegativity differences (Ref. 40).

^h Values from bulk compound.

ⁱ Estimations based only on bulk compounds binding energies.

configuration is much more similar to that of a rare-gas atom. This is, in fact, supported by the observation of spectral terms which can be scaled to those of the nearest rare gas. Therefore, it is likely that the chemisorbed atom is in the form of an ion. We argue, in the following, that $\mathcal{F} - R_a$ is given by the total energy shift, ΔE_{mo1} , of the Auger peak of a molecule of the compound adsorbate-hydrogen.

We discuss first the case of oxygen chemisorbed on copper. In Fig. 9 we have represented the values of ΔE_{mo1} corresponding to the four most intense spectral terms (1D for the $KL_{23}L_{23}$, 3P and 1P for the KL_1L_{23} , and 1S for the KL_1L_1 transitions) of HF, H_2O , and CH_4 molecules as a function of the corresponding values, ΔE_{Ne} , for neon atoms. ΔE_{mo1} are calculated from Eq. (3) using available data for HF, $^{30}H_2O$ (XPS, $^{37}AES^{24}$), and CH_4 (XPS, $^{37}AES^{36}$) molecules. It is observed that the HF and H_2O plots can be fitted in good approximation by straight lines passing through the origin,

the maximum deviation not exceeding 0.5 eV. A least-squares fitting of the data gives slopes of 0.82 and 0.70, respectively. In the limit of perfect ionicity, the electron configurations of HF and H_2O correspond to a rare gas and no extra-atomic relaxation is, therefore, expected. This agrees with the observation of both lines going through the origin. The decreasing slope in the series Ne, F^- , O^{2-} reflects the decreasing positive charge of the ion cores. Physically, one can visualize a less positive core as giving rise to a lesser binding and, consequently, to a looser $2p$ configuration resulting in a decreased effective hole-hole interaction ($\mathcal{F} - R_a$).

Oxygen in our chemisorbed layers is likely to have the same electron configuration of Ne, F^- , and O^{2-} . Moreover, its ion core is very similar to that of a water molecule. Therefore, it is expected that its intra-atomic contribution to ΔE ($\mathcal{F} - R_a$), is very similar to ΔE_{mol} of water. This is indeed confirmed by Fig. 9, in which ΔE for

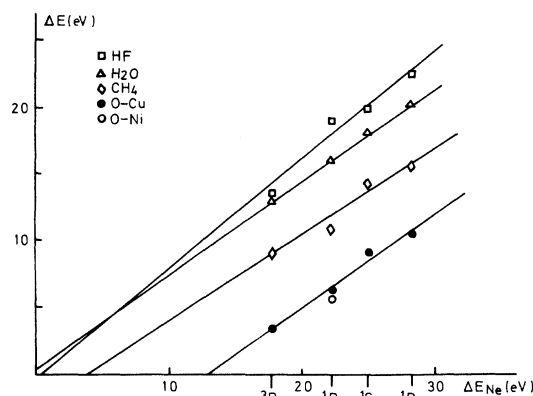


FIG. 9. Energy shifts ΔE associated to the different spectral terms appearing in the $KL_{23}L_{23}$ spectra of HF, H_2O , and CH_4 gas molecules and of oxygen chemisorbed on copper and nickel as a function of the corresponding shift ΔE_{Ne} in the neon atom. Straight lines have been least-square fitted to the results as discussed in the text.

oxygen on copper is also plotted as a function of ΔE_{Ne} . If a straight line is least-square fitted to the data, the resulting slope, 0.70, is equal within experimental error to that of water. On the other hand, the line is displaced downwards by an amount of 9.4 eV. According to Eq. (4) this is the value of R_e . An upper bound for the error of ± 0.9 eV is obtained by letting the ΔE values shift to their most deviated values (according to estimations above) and calculating then the mean-square error associated to the plot ΔE_{mol} vs ΔE_{Ne} .

For the system oxygen on nickel, the points in a ΔE vs ΔE_{Ne} diagram show a greater dispersion. We prefer to rely only on the ΔE value corresponding to the 1D term, because it has been obtained through photoemission data of chemisorbed layers. If we assume the same slope that for H_2O and oxygen on copper, one gets $R_e = 10.2$ eV. An upper error of ± 1.5 eV is obtained by just adding the uncertainty in the position of $E(jkl)$ to the error in the O-Cu system.

In order to obtain ΔE for sulphur on nickel, one requires the values of $\mathcal{F} - R_a$ for a sulphur adsorbate. Unfortunately, experimental Auger data for gas molecules of hydrogen sulfide are not available. A rough estimation may be obtained by the following method: For an atom ΔE_{at} is just given by

$$\Delta E_{at}(kk, Y) = \mathcal{F}(kk, Y) - R_a = E_{at}(kk, Y) - 2E_{at}(k), \quad (8)$$

where $E_{at}(kk, Y)$ is the binding energy of a double hole in level k . Values of ΔE_{at} for the elements can, then, be computed from double ionization data.³⁹ Values of ΔE_{at} for elements of the 2nd and 3rd row are shown in Fig. 10. The ones of the 2nd row are compared to ΔE_{mol} associated to the

1D spectral terms of the corresponding p^4 final configuration. It is clear that the apparent anomaly of oxygen (due to the high-energy necessary to break the highly stable spin configuration in the p^3 single ionized state) is corrected when going to the O^{--} case. It is worth remarking that the experimental value for O^{--} falls fairly on the slowly monotonically decreasing curve of ΔE_{at} for the elements. Comparison of the data for the 2nd and 3rd row allows one to estimate a value of $\mathcal{F}(M_{23}M_{23}, ^1D) - R_a(MM) \approx 10$ eV for a sulphur ion. This results in $R_e \approx 6.7$ eV for sulphur on nickel. The case of sulphur on iron is less reliable because even the ΔE values for 1D terms are evaluated for M_{23} levels corresponding to bulk material. All these values of R_e are included in Table VII, the ones in brackets being considered only as indicative. The values of R_e range from ~ 5 to ~ 10 eV. In the last column of that table, the ionicity of the compound, as evaluated from differences in electronegativities,⁴⁰ has been included. The results seem to suggest that higher relaxation energies R_e are present when the degree of ionicity of the bond increases but no quantitative conclusion is justified on the basis of the present data. This is mostly due to uncertainties in the binding and intraatomic relaxation energies, that have been used in the estimation of R_e .

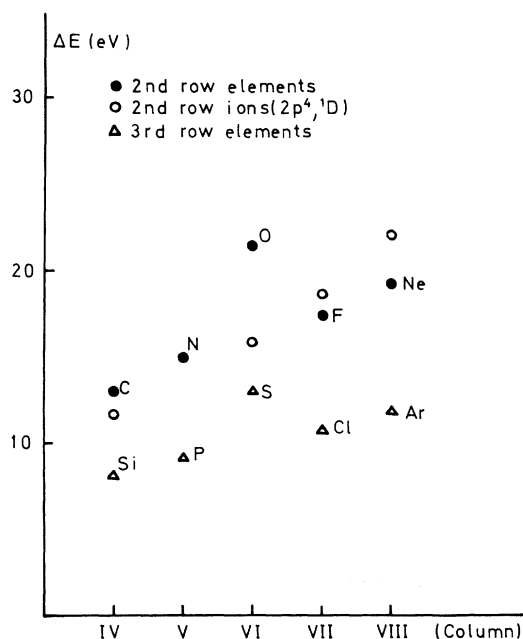


FIG. 10. Intraatomic contribution, $\Delta E_{at} = \mathcal{F} - R_a$, for several atoms in columns IV–VIII and rows 2 and 3 of the periodic system. The data correspond to atoms in neutral (\bullet, Δ) (highest spectral term) and fully ionized (\circ) (rare gas atom p^6 configuration, 1D spectral term) form. For neon, both values are connected to 3P and 1D spectral terms.

V. AUGER SPECTRA LINE SHAPE AND DENSITY OF STATES

The discussion of Sec. IV has shown that the fine structure of their Auger spectra is closely related to the electronic structure of materials. A most important question is whether or not the DOS can be obtained by analyzing the line shape of Auger spectra involving one or two holes in the valence band. We assume here that complications arising from nonconstant matrix elements have been adequately dealt with and discuss only the range of validity of Eqs. (5) and (6). As indicated in Sec. IV A, previous investigations show that the latter equations can be used in a variety of cases, all of which have in common the property of involving quasi-free-electrons in the band. We discuss now the possibility of relating AES to the DOS in the case of valence bands consisting of rather localized electrons. We propose that, in this case, AES line-shape measurements can be used for obtaining information about DOS if only interatomic transitions are taken into account. There are, at least, four types of results on which this proposition is founded: (i) Observation of a d -band peak X_1 in Auger spectra of adsorbate gases on transition metals. As discussed in Sec. IV C this peak appears in a position associated to an unshifted d band; (ii) observation of a large interatomic peak in magnesium oxide, whose deconvolution closely resembles the DOS by soft-x-ray emission spectroscopy (SXS); (iii) AES investigations of copper and nickel, in which a small peak corresponding to the unshifted position of the d band of the metal is observed; and (iv) INS data on copper and nickel.

The term DOS is used here in a sense that is worth fixing precisely. The term local density of states (LDOS) has been coined with the purpose of dealing with the variations from cell to cell of the bulk density of states in the proximity of crystal discontinuities, for example surfaces. The concept of LDOS can be extended in order to describe local variations of the effective density of states from one point of the cell to another. For example, in transition metals, tight-binding d -band wave functions tend to be more concentrated around the atom cores than nearly-free-electron s -band wave functions. Therefore, the d -band contribution to the LDOS, in the present sense, is much more pronounced in the core region than near the corners of the cell. According to this picture, we may say that AES (and SXS) *do not* sample the same LDOS as do INS, XPS, or UPS. Earlier comparisons between AES and XPS have been interpreted along these lines.⁷ These ideas are also relevant in connection with interatomic transitions, and, in fact, a somehow physically equivalent problem

has been treated in detail by Hagstrum¹⁶ in connection with the quantity that is actually sampled by INS. According to the terminology of the latter, interatomic transitions give only a transition density function. Nevertheless, comparison of this quantity with other probes of density of states (for example, comparing INS data with electron-loss spectroscopy for the same system⁴¹) suggests that no substantial differences exist between both functions.

The microscopic description of the mechanism by which the initial hole perturbs the DOS in intra-atomic transitions is not clear at the moment. On the other hand, there are certain observations that are rather intriguing. Particularly, the comparison between SXS and intra-atomic AES spectra remains an open question. Both techniques have an initial core hole and, consequently, should be subjected to the same perturbation. However, SXS is known to give results directly related to the DOS,^{42,43} whereas perturbation effects in AES have been shown to be strong. It has been argued¹¹ that lifetimes of core holes are longer for x-ray emission and, therefore, that relaxation of the Fermi sea around the hole would be more complete. However, this explanation is untenable because photon and Auger emission are processes competing for the inner hole deexcitation and it is well known that, in such a case, the lifetime of the hole would be controlled by the fastest one.

It is unfortunate that for most adsorption systems studied here, interatomic peaks in Auger spectra are rather weak. This makes it difficult to use them in order to get information about the DOS. Of course, when the electronic structure is such that competitive intra-atomic transitions are unlikely (as in AES of magnesium oxide or in INS), suitable treatment of the results, such as self-deconvolution and allowance for transition-matrix modulation effects, should result in DOS information. However, this situation is seldom attained and very good resolution and sensitivity are, in any case, required. It is also worth remarking that no interatomic transition in the metal substrate peak, arising from electrons in the upper levels of the adsorbate, has been yet detected. A number of reasons for this absence may be suggested. One is related to the fact that the high number of electrons in the metal valence band make deexcitations involving extraatomic levels very unlikely. This is supported by the small intensity of the proposed interatomic peak in pure metals.¹⁴ The deexcitation of a substrate hole via electrons coming from the adsorbate atoms is still less probable on the basis of an argument based on the number of neighboring electrons. Experiments to check these ideas are being carried out in our laboratory at present.

VI. CONCLUSIONS

Two major conclusions can be drawn from the present work. The first is that AES, apart from its well established application for the determination of surface composition, can be considered as a valence-band spectroscopy, capable of providing detailed knowledge of the electronic structure near the surface. This knowledge includes information about the LDOS, which, under certain circumstances, is comparable and somehow complementary to the ones obtained by more conventional techniques such as photoemission. Concerning the interpretation of fine structure in Auger spectra of adsorbate layers, it is demonstrated that two different types of transition, intra-atomic and interatomic, contribute to those spectra and that careful distinction between the two is necessary in order to make a sound interpretation of experiments. Particularly, interatomic transitions are shown to provide information about the LDOS, even for such systems in which earlier investigations had shown the Auger main

peak to be quasiatomic in character.

The second conclusion is that the analysis of Auger spectra can provide additional information concerning the bonding near the surface in the form of relaxation energies, degree of ionicity, etc. Information about relaxation energies, and associated energy shifts in the spectra, are most important as it becomes more and more clear that the interpretation of experimental data on electronic levels (for example, from photoemission) can be seriously misleading if these effects are not accounted for.

ACKNOWLEDGMENTS

We thank Mr. S. Ferrer for providing his data concerning zinc substrates, Dr. E. N. Sickafus for awakening our interest in this problem, and Professor N. Cabrera for continuous stimulation and advice. Part of this work was performed with financial help from an A. T. P. of the C. N. R. S. that we gratefully acknowledge.

*Centro Coordinado C. S. I. C.-U. A. M.

¹J. J. Lander, Phys. Rev. 91, 1382 (1953).

²G. F. Amelio and E. J. Scheibner, Surf. Sci. 11, 242 (1968).

³G. F. Amelio, Surf. Sci. 22, 301 (1970).

⁴R. G. Musket and R. J. Fortner, Phys. Rev. Lett. 26, 80 (1971).

⁵C. J. Powell, Phys. Rev. Lett. 30, 1179 (1973).

⁶E. N. Sickafus, Phys. Rev. B 7, 5100 (1973).

⁷J. Tejada, M. Cardona, N. J. Shevchik, D. W. Langner, and E. Schönherr, Phys. Status Solidi B 58, 189 (1973).

⁸S. Ferrer, A. M. Baró, and M. Salmerón, Solid State Commun. 16, 651 (1975).

⁹A. J. Jackson, C. Tate, T. E. Gallon, P. J. Bassett, and J. A. D. Matthew, J. Phys. F 5, 363 (1975).

¹⁰S. P. Kowalczyk, R. A. Pollak, F. R. McFeely, L. Ley, and D. A. Shirley, Phys. Rev. B 8, 2387 (1973).

¹¹L. O. Yin, I. Adler, T. Tsang, M. H. Chen, D. A. Ringers, and B. Crasemann, Phys. Rev. A 9, 1070 (1974).

¹²C. J. Powell and A. Mandl, Phys. Rev. Lett. 29, 1153 (1972).

¹³P. J. Bassett, T. Gallon, J. A. D. Matthew, and M. Prutton, Surf. Sci. 35, 63 (1973).

¹⁴A. M. Baró, M. Salmerón, and J. M. Rojo, J. Phys. F 5, 826 (1975).

¹⁵M. Salmerón, A. M. Baró, and J. M. Rojo, Surf. Sci. 53, 689 (1975).

¹⁶H. D. Hagstrum, Phys. Rev. 150, 495 (1966).

¹⁷M. Salmerón and A. M. Baró, Surf. Sci. 49, 356 (1975).

¹⁸S. P. Kowalczyk, L. Ley, F. R. McFeely, R. A. Pollak, and D. A. Shirley, Phys. Rev. B 9, 381 (1974).

¹⁹H. Körber and W. Mehlhorn, Z. Phys. 191, 217 (1966).

²⁰W. Mehlhorn and D. Stahlherm, Z. Phys. 217, 294 (1968).

²¹W. N. Asaad and E. H. S. Burhop, Proc. Phys. Soc.

Lond. 72, 369 (1958).

²²D. A. Shirley, Phys. Rev. A 7, 1520 (1973).

²³H. D. Hagstrum and G. E. Becker, Phys. Rev. Lett. 16, 230 (1966).

²⁴W. E. Moddeman, T. A. Carlson, M. O. Krause, B. P. Pullen, W. E. Bull, and G. K. Schweitzer, J. Chem. Phys. 55, 2317 (1971).

²⁵D. G. Lord and T. E. Gallon, Surf. Sci. 36, 606 (1973).

²⁶P. J. Bassett, T. E. Gallon, M. Prutton, and J. A. D. Matthew, Surf. Sci. 33, 213 (1972).

²⁷P. H. Citrin, J. Electron. Spectrosc. 5, 273 (1974).

²⁸T. Kawai, K. Kunimori, T. Kondow, T. Onishi, and K. Tamaru, Phys. Rev. Lett. 33, 533 (1974).

²⁹P. H. Citrin, P. M. Eisenberger, W. C. Marra, T. Alberg, J. Utraiainen, and E. Källne, Phys. Rev. B 10, 1762 (1974).

³⁰R. W. Shaw, Jr., and T. D. Thomas, Phys. Rev. A 11, 1491 (1975).

³¹T. B. Grimley, in *Molecular Processes on Solid Surfaces*, edited by E. Drauglis, R. D. Gretz, and R. I. Jaffee (McGraw-Hill, New York, 1969), p. 299.

³²J. E. Houston, R. L. Park, and G. E. Laramore, Phys. Rev. Lett. 30, 846 (1973).

³³H. D. Hagstrum and G. E. Becker, J. Chem. Phys. 54, 1015 (1971).

³⁴S. Hüfner and G. K. Wertheim, Phys. Rev. B 8, 4857 (1973).

³⁵D. E. Eastman and J. K. Cashion, Phys. Rev. Lett. 27, 1520 (1971).

³⁶S. Ohtani, K. Terada, and Y. Murata, Phys. Rev. Lett. 32, 415 (1974).

³⁷K. Siegbahn, C. Nordling, G. Johansson, J. Hedman, P. F. Heden, K. Hamrin, U. Gelius, T. Bergmark, L. O. Werme, R. Manne, and Y. Baer, *ESCA Applied to Free Molecules* (North-Holland, Amsterdam, 1969).

³⁸R. Spohr, T. Bergmark, N. Magnusson, L. O. Werme, C. Nordling, and K. Siegbahn, Phys. Scr. 2,

- 31 (1970).
- ³⁸C. E. Moore, *Atomic Energy Levels*, Natl. Bur. Stand. Special Circular No. 467 (U. S. GPO, Washington, D. C., 1949), Vols. I-III.
- ⁴⁰L. Pauling, *The Nature of the Chemical Bond* (Cornell University, Ithaca, 1960).
- ⁴¹F. Steinrisser and E. N. Sickafus, *Phys. Rev. Lett.* 27, 992 (1971).
- ⁴²J. R. Cuthill, A. J. McAlister, M. L. W. Williams, and R. E. Watson, *Phys. Rev.* 164, 1006 (1967).
- ⁴³C. Sugiara, Y. Gohshi, and I. Suzuki, *Phys. Rev. B* 10, 338 (1974).